Neotropical Ichthyology

Original article

https://doi.org/10.1590/1982-0224-2022-0072

Morphometric and molecular differentiation of *Pimelodus grosskopfii* and *Pimelodus yuma* (Siluriformes: Pimelodidae)

Correspondence:
Edna Judith Márquez
ejmarque@unal.edu.co

Cristhian Danilo Joya[1], Ana María Ochoa-Aristizábal[1], José Gregorio Martínez[1,2] and Edna Judith Márquez[1]

Pimelodus grosskopfii and *Pimelodus yuma*, two species endemic to the Magdalena-Cauca basin in Colombia, overlap in the ranges of some of their diagnostic characters, which hampers their correct morphological identification. Aiming to help discriminate these species, this study conducted an integrative analysis using traditional and geometric morphometrics, phylogenetic analysis based on partial sequences of the mitochondrial *cytochrome c oxidase subunit 1* gene (COI, *cox1*) and the identification of diagnostic Single Nucleotide Polymorphism markers (SNP). The species differ significantly in body geometry, allowing 100% discrimination, which was reinforced by a phylogenetic analysis that recovered well-supported monophyly of each species (posterior probability > 0.95). Additionally, the traditional morphometric results corroborated some previously reported diagnostic traits for both species and let us describe one non-overlapping ratio related to the adipose fin length. Three of five SNP markers had reciprocally exclusive alleles suitable for identifying each species. The morphometric and molecular methods conducted in this study constitute alternative tools for the correct discrimination of *P. grosskopfii* and *P. yuma* in the wild and in captive populations used for aquaculture.

Keywords: Phylogenetic analyses, Freshwater fishes, Shape variation, SNPs markers, Cox1.

Submitted July 17, 2022
Accepted April 20, 2023
by Brian Sidlauskas
Epub May 29, 2023

Online version ISSN 1982-0224
Print version ISSN 1679-6225

Neotrop. Ichthyol.
vol. 21, no. 2, Maringá 2023

1 Facultad de Ciencias, Escuela de Biociencias, Laboratorio de Biología Molecular y Celular. Carrera 65 No. 59A – 110 Bloque 19A, Laboratorio 310, Universidad Nacional de Colombia – Sede Medellín, Medellín 050034, Colombia. (CDJB) cdjoyab@unal.edu.co, (AMOA) aochoaa@unal.edu.co, (EJM) ejmarque@unal.edu.co (corresponding author).

2 Facultad de Ciencias de la Salud, Grupo de Investigación Biociencias, Institución Universitaria Colegio Mayor de Antioquia, Medellín, Colombia. (JGM) jose.martinez@colmayor.edu.co.

Pimelodus grosskopfii y *Pimelodus yuma*, dos especies endémicas de la Cuenca Magdalena-Cauca en Colombia, se superponen en los rangos de variación de algunos de sus caracteres diagnósticos, lo que dificulta su correcta diferenciación morfológica. Con el objetivo de contribuir a la discriminación de estas especies, se realizó un análisis integrativo utilizando la morfometría geométrica y tradicional, análisis filogenético basado en secuencias parciales del gen mitocondrial *citocromo c oxidasa* subunidad I (COI, *cox1*) y la identificación de marcadores diagnósticos de polimorfismo de nucleótido único (SNP). Las especies difieren significativamente en la geometría del cuerpo, permitiendo una discriminación del 100%, lo que fue reforzado por un análisis filogenético que recuperó una monofilia bien soportada para cada especie (probabilidad posterior > 0,95). Además, los resultados de la morfometría tradicional corroboraron algunos rasgos diagnósticos previamente reportados para ambas especies y nos permitieron describir una proporción que no se sobrepone, relacionada con la longitud de la aleta adiposa. Tres de los cinco marcadores SNP poseían alelos recíprocamente exclusivos, adecuados para identificar cada especie. Los métodos morfométricos y moleculares implementados en este estudio constituyen herramientas alternativas para la correcta discriminación de *P. grosskopfii* y *P. yuma* tanto en la naturaleza como en poblaciones cautivas utilizadas para la acuicultura.

Palabras clave: Análisis filogenético, Peces de agua dulce, Variación de conformación Marcadores SNPs, Cox1.

INTRODUCTION

Pimelodidae is one of the most diverse Neotropical families within the order Siluriformes, comprising 30 genera and 116 species (Fricke *et al*., 2022a) distributed from Panama to South America (Nelson *et al*., 2016). Members of this family are economically important and highly demanded in commercial fisheries and in the ornamental fish trade (Cala-Cala, 2019). Within Pimelodidae, *Pimelodus* Lacepède, 1803 includes 36 valid species (Fricke *et al*., 2022b), three of which are endemic to the colombian Magdalena-Cauca basin: 1) *Pimelodus crypticus* Villa-Navarro & Cala, 2017, restricted to the upper Cauca River drainage; 2) *Pimelodus yuma* Villa-Navarro & Acero, 2017, distributed in the Magdalena, Cauca and Sinú river drainages, and 3) *Pimelodus grosskopfii* Steindachner, 1879 which inhabits the Magdalena-Cauca basin. *Pimelodus crypticus* and *P. yuma* are recently recognized species that had been subsumed within the concept of *Pimelodus blochii* Valenciennes, 1840 (Villa-Navarro *et al*., 2017).

Pimelodus grosskopfii and *P. yuma* occur sympatrically in the lower Cauca and Magdalena River basins, where they migrate up to 500 km (Zapata, Usma, 2013). Both species reproduce externally and are omnivorous with insectivorous preferences (Lasso *et al*., 2011; Ramírez, Pinilla, 2012), although Jiménez-Segura *et al*. (2020) considered *P. yuma* to be carnivorous. Both congeners are among the top five species of fishery interest (Hernández-Barrero *et al*., 2020) and exhibit two genetic stocks in the lower section of the Cauca River (Joya *et al*., 2021; Restrepo-Escobar *et al*., 2021). The International

Union for Conservation of Nature – IUCN lists *P. grosskopfii* as Critically Endangered (CR), whereas *P. yuma* has not yet been included or evaluated (Villa-Navarro *et al*., 2016).

Overlapping ranges in some diagnostic characters hamper the correct morphological identification of *P. grosskopfii* and *P. yuma*. Additionally, phenotypic plasticity influences some traits that putatively discriminate *P. grosskopfii* from *P. yuma*, which could hinder the correct identification of both species. The potentially plastic traits include the dark spots along the entire length of the body, longer adipose fin, and shorter distance between the dorsal and adipose fins in *P. grosskopfii* (Villa-Navarro *et al*., 2017). For instance, body coloration in fishes can change in response to light (Ninwichian *et al*., 2018; Pinto *et al*., 2020) or other external environmental stimuli (Sugimoto, 2002; Van Der Salm *et al*., 2004), or to enhance reproduction or survival (Rodgers *et al*., 2010). Biotic and abiotic conditions and metabolic requirements can affect the size and presence of the adipose fin in some catfish species (Reimchen, Temple, 2004; Temple, Reimchen, 2008). Variation in water velocity is known to induce body shape variation in *P. grosskopfii* (Hincapié-Cruz, Márquez, 2021). Thus, the ability of morphological characteristics to diagnose these similar species may be questioned.

In this context, the present study assessed the utility of four approaches to discriminate between the catfish species *P. grosskopfii* and *P. yuma*: traditional and geometric morphometrics, phylogenetic analysis of a portion of the mitochondrial *cox1* gene, and identification of diagnostic single nucleotide polymorphisms (SNPs) in the nuclear genome. Traditional morphometrics quantify a series of morphological characters (length, depth, and width; or their expression as means, ranges, or ratios) and use multivariate methods that allow describing patterns of variation (Marcus, 1990; Rohlf, Marcus, 1993). Together with meristic characters (*e.g*., Londoño-Burbano *et al*., 2011; Vanegas-Ríos *et al*., 2011; Arcila *et al*., 2013; Ferrer, Malabarba, 2013), and geometric morphometric data (*e.g*., Maderbacher *et al*., 2008; Sidlauskas *et al*., 2011; Gupta *et al*., 2018; Garavello *et al*., 2021), the morphological characters are widely used for identifying neotropical fish species. Geometric morphometrics allows the analysis of biological shape variation and its covariance with other variables and thus can find patterns of morphological variation among and within species (Bookstein, 1992). In fishes, this method can discriminate morphologically similar species (García-Alzate *et al*., 2011), assess sexual dimorphism (Herler *et al*., 2010), test the covariation of shape with environmental conditions (Restrepo-Escobar *et al*., 2016a,b; Hincapié-Cruz, Márquez, 2021) and support studies of genetic differentiation (Kocovsky *et al*., 2013).

Partial sequences of the mitochondrial gene *cox1* are often used as a barcode to differentiate animal species (Hebert *et al*., 2003) due to their wide availability in public databases (Heller *et al*., 2018) and other advantages of mitochondrial DNA (mtDNA) such as the simple structure, high copy number, uniparental inheritance, and rapid evolutionary rate (Rubinoff, Holland, 2005). This gene has successfully discriminated freshwater fish species from Canada (Hubert *et al*., 2008), Central America (Valdez-Moreno *et al*., 2009), and Taiwan (Bingpeng *et al*., 2008). It has also performed well in several studies of *Pimelodus* in South America (Rosso *et al*., 2012; Becker *et al*., 2015; Frantine-Silva *et al*., 2015; Díaz *et al*., 2016; Guimarães-Costa *et al*., 2019).

However, *cox1* sequences do not diagnose all species reliably; given the uniparental inheritance of mtDNA, this gene cannot elucidate hybridization or introgression events (Hubert *et al*., 2008). Thus, this study also explored the utility of SNPs in nuclear genes

by taking advantage of a RAD-seq library of previously *cox1* barcoded individuals of *Pimelodus* (Martínez *et al*., 2022). Although closely related species will not have diverged at all genomic regions (Duranton *et al*., 2018), the occurrence of genomic islands, intraspecific selection (Duranton *et al*., 2018), and random fixation of alleles by mutation-drift equilibrium (Martin, Jiggins, 2017) usually result in rapid divergence and fixation of diagnostic alleles at some loci. Such exclusive regions are the target for the development of SNPs markers employed to discriminate *P. grosskopfii* from *P. yuma*.

The present study explores the utility of morphometric and molecular tools to discriminate these catfish species. Reliable diagnoses would aid in identifying individuals from wild or farmed populations to the correct species and help to scaffold further interspecific genetic analyses.

MATERIAL AND METHODS

Sampling. A total of 159 *cox1* barcoded individuals of the genus *Pimelodus* from the Magdalena and Cauca rivers were analysed (Fig. 1, Tabs. **S1** and **S2**). A subgroup of 125 samples from the middle and lower sector of the Cauca River and lower sector of the Magdalena River (Tab. **S1**) was evaluated by phylogenetic and morphometric analyses, while the remaining 34 samples from a previously sequenced RAD-seq library (Martínez *et al*., 2022) were used for genome association studies. This last subgroup also included samples from the upper sectors of Cauca and Magdalena rivers (Tab. **S2**).

Traditional and geometric morphometrics. A total of 125 individuals (79 females and 46 males) were photographed in left lateral view within a diffuse light box at 0.47 m focal length using a dual pixel 12 MP Samsung digital camera. The sex identification was based on the usual method of applying external abdominal pressure to obtain gametes in ripe adults and visual inspection of the urogenital papillae (Ross, 1984). Digitization of landmarks was conducted using the online application XYOM v. 2.0 (Dujardin, Dujardin, 2019; https://xyom.io/). For each image, nine landmarks were digitalized (Fig. 2): eight type I (juxtaposition of tissues) and one type II (point of maximum curvature in the head; Bookstein, 1992).

To ensure maximum precision in landmark assignment, digitization was repeated twice, and the repeatability index was quantified using XYOM v. 2.0. Centroid size (CS) was calculated based on landmark coordinates (x, y), and then a Generalized Procrustes Analysis was conducted to eliminate shape variation resulting from differences in size, position, and rotation. Finally, the partial (partial warps) and global (uniform components) shape deformations of individuals with respect to the consensus (Goodall, 1991; Warheit *et al*., 1992) were used as shape variables.

Differences in body shape between species and sexes were explored using a Principal Components Analysis (PCA), and the statistical significance of Euclidean distances among groups was obtained by 1,000 permutations. In addition, the allometric effect was calculated using a multivariate regression between shape variables and centroid size. When significant allometry was detected, a size correction of shape was conducted if allometric slopes fit a common model, which was assessed using a Multivariate Analysis of Covariance (MANCOVA). Additionally, the diagnosability of each group suggested

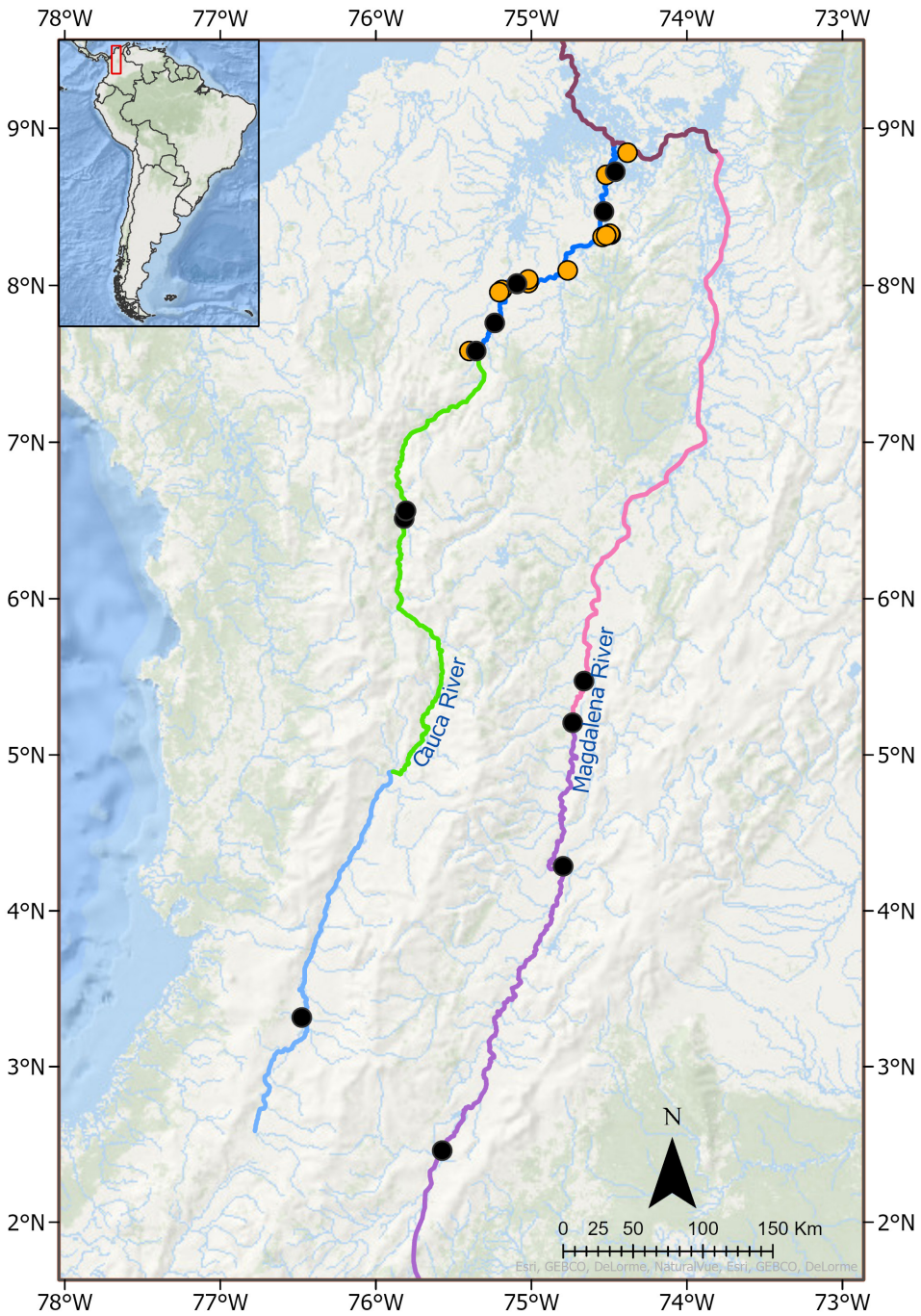

FIGURE 1 | Sampling sites of *Pimelodus grosskopfii* and *P. yuma* in the Cauca and Magdalena rivers. Orange circles: samples submitted to geometric morphometric and phylogenetic analyses; black circles: samples used for identification of diagnostic SNPs. Light blue, light green, dark blue: upper, middle, and lower section of the Cauca River, respectively; light purple, pink, dark purple: upper, middle, and lower section of the Magdalena River, respectively.

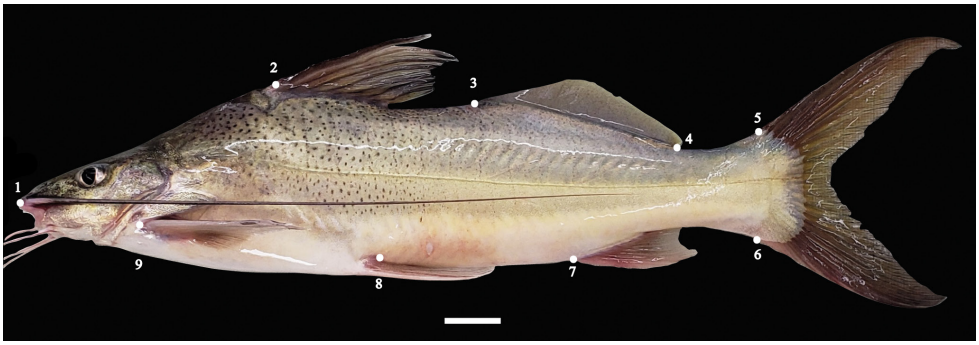

FIGURE 2 | Landmarks used for morphometric analysis of *Pimelodus grosskopfii* (photo) and *P. yuma*: 1, tip of the snout; 2, dorsal-fin origin; 3–4, adipose-fin origin and insertion, respectively; 5–6, origin of posterior most dorsal and ventral caudal-fin rays; 7, anal-fin origin; 8, pelvic-fin origin; 9, pectoral-fin origin. Scale bar = 1 cm.

by PCA was examined via assignment tests using Simple Reclassification and Verified Cross-Classification. All calculations were conducted in XYOM v. 2.0.

To assess differences in centroid size, we conducted a pairwise Tukey's test among compared groups and a two-way ANOVA including groups and sex as main factors. This analysis was performed after verifying that the centroid size met the assumptions of normality (Shapiro-Wilks test) and homoscedasticity (Levene's test with the Brown-Forsythe modification) using, respectively, the packages nortest v. 1.0.4 and stats v. 3.6.0, of the statistical program R (R Development Core Team, 2013).

Finally, we calculated distances between landmarks to obtain traditional morphological data from all 125 photographs and visualized differences among individuals by PCA. The numbers of pixels were converted into centimetres using a reference scale within each image, then transformed using the Neperian logarithm. Because standard length was not directly measured in our landmark set, we approximated that measure as the mean of the distances between the tip of the snout and the dorsal and ventral origins of the caudal fin. All other measurements were then expressed as percentage of the approximated standard length. The measurements that displayed a greater contribution to the total variation were evaluated by parametric (t tests, if assumptions of normality and homoscedasticity were met) or non-parametric tests (Welch t-test, Kruskal-Wallis, and Mann-Whitney test) using the stats package v. 3.6.3 implemented in R. The ratio distance/length of the adipose fin was also calculated to explore whether that ratio can discriminate the species. To assess possible allometric variation in that ratio, the ratio of the distance/length of the adipose fin was regressed on standard length using standardized major axis regression in smatr v. 3.4-8 of the statistical program R (R Development Core Team, 2013).

Phylogenetic analyses. DNA extraction was performed from 125 fin or muscle tissues previously preserved in 96% ethanol using the GeneJET Genomic DNA Purification kit, following the manufacturer's instructions. A partial region of the mitochondrial *cox1* gene was amplified using a cocktail of four primers: VF2_t1 5'-TCAACCAACCACAAAGACATTGGCAC-3', FishF2_t1 5'-TCGACTAATCATAAAGATATCGGCAC-3', FishR2_t1

5'-ACTTCAGGGTGACCGAAGAATCAGAA-3' (Ward *et al*., 2005) and FR1d_t1 5'CACCTCAGGGTGTCCCGAARAAYCARAA-3' (Ivanova *et al*., 2007). Polymerase chain reactions (PCR) were implemented in a total volume of 30 µL containing 5-20 ng/µl of genomic DNA, 1X of PCR buffer, 2.5 mM of $MgCl_2$ 50 mM, 0.25 mM of dNTPs mix 10 mM, 0.2 pmol/µL of the primer cocktail and 0.025 U/µl of Platinum Taq DNA polymerase. The thermal profile consisted of a first denaturation step at 95°C for 3 min followed by 32 cycles at 94 °C for 30 sec, 35 sec at 60 °C and 30 sec at 72 °C, using a final extension at 72 °C for 3 min. PCR products were confirmed by 1.5% agarose gel electrophoresis and EZ vision staining, and sequencing was performed on an ABI 3730XL automated sequencer. The forward and reverse sequences were inspected using Geneious v. 11.0.4 (https://www.geneious.com). Sequence editing and alignment (ClustalW algorithm) to generate a consensus sequence were conducted in Bioedit v. 7.0.9.0 (Hall, 1999). The software Geneious v. 11.0.4 was also used to translate consensus sequences into the corresponding amino acids to confirm the absence of stop codons or frame shift errors within the sequence.

The number of haplotypes, nucleotide diversity (π) and haplotype diversity (Hd) were calculated in DNAsp v. 6 (Rozas *et al*., 2017). The best fit model of molecular evolution was selected using jModelTest v.2.1.10 (Guindon, Gascuel, 2003; Darriba *et al*., 2012). Haplotypes obtained in this study were compared with known *cox1* sequences from *Pimelodus crypticus* (OK206769; ON596099), *P. grosskopfii* (MK748281) and *P. yuma* (NC_061908). In addition, a previously published GenBank sequence of *Pseudoplatystoma magdaleniatum* Buitrago-Suárez & Burr, 2007 (KP090204) was used as outgroup. Phylogenetic analysis was conducted in BEAST v. 2.6.4 (Bouckaert *et al*., 2019) implemented on the CIPRES Science Gateway (available at http://www.phylo.org/). To this end, an xml file was created in BEAUti, setting HKY + G as the best-fit model, a strict molecular clock with a clock rate of 1 and a Yule model as a prior on the speciation process; remaining parameters were left at their default settings. Analyses were performed using 900 million Markov Monte Carlo Chains (MCMC) sampled every 90,000 generations, and discarding the initial 10% as burn-in. Convergence (ESS value > 200) was assessed using Tracer v. 1.7 (Rambaut *et al*., 2018) and a consensus tree was generated using Treeannotator v. 1.10.4. Finally, the obtained phylogenetic tree was visualized using Fig Tree (http://tree.bio.ed.ac.uk/). Following Hubert *et al*. (2008) recommendations for the DNA barcoding of freshwater fishes, the haplotypic divergences between and within species was estimated by calculating the Kimura 2 parameter model in Mega v. 11.0.13 (Tamura *et al*., 2021). For species discrimination based on PCR methods, two primer pairs were designed using Primer-Blast (which in turn uses Primer3, Untergasser *et al*., 2012) to design PCR primers and BLAST and global alignment algorithm to screen non-specific amplifications of primer pairs against a user-selected database (Ye *et al*., 2012). The same approach was used for designing primers for diagnostic SNP loci identified as described below.

Identification of diagnostic SNPs. Reads of 34 *cox1* barcoded individuals of *Pimelodus* (24 *P. grosskopfii*, 10 *P. yuma*; ON596146 – ON596170; OK206803, OK206739, OK206761, OK206705, OK206706, OK206726, OK206728, OK206800, OK206804) were obtained from a RAD-seq library (restriction enzyme *PstI*, sonication) previously sequenced on the Illumina HiSeq 2000 platform at Floragenex Inc. (USA) (Martínez

et al., 2022). To produce a catalogue of RADseq tag loci, alleles, and single nucleotide polymorphisms (SNPs) from the raw NGS reads, we used the software RADproc v. 3 (Ravindran *et al*., 2019) to demultiplexing by 16-nt barcodes, filter the samples by quality and construct *de novo* loci. The script used the following parameters: "-*a*" *psweep* mode for loci assembling optimization, Phred score threshold >20, minimum sequencing depth of 3 (-*m*), maximum allowed distance (in nucleotides) among stacks of 4 (-*M*), maximum allowed distance among putative loci of 1 (-*n*), maximum stacks per locus of 2 (-*x*) and minimum percentage of samples of 0.9 (-*S*).

The SNP output files for population analyses (STRUCTURE and VCF) were generated by STACKS v. 2.53 (Catchen *et al*., 2013) from the RADproc catalogues, running the modules SSTACKS, TSV2BAM, GSTACKS, and POPULATIONS in pipeline mode. In the STACKS map file, each individual was considered as a population; in the POPULATIONS module, the minimum number of populations was set to 100%, the minimum percentage of individuals in a population required to process a locus for that population was set to 90% (-r = 0.9), with a minor allele frequency (MAF) of 0.05, and remaining parameters were left by default.

To corroborate the existence of *P. yuma* and *P. grosskopfii* as biological entities for subsequent population analyses, a coancestry analysis was performed in STRUCTURE v. 2.3.4 (Pritchard *et al*., 2000) using 20 independent runs from K = 1 to K = 4, 1,000,000 Markov Monte Carlo Chains (MCMC) and a burn-in of 100,000 iterations; STRUCTURESELECTOR (Li, Liu, 2018) was used to calculate the best estimate of K. A summary of structure runs was plotted on a coancestry histogram of all individuals using the integrated software CLUMPAK (Kopelman *et al*., 2015).

Once the biological assignation of the 34 individuals was corroborated, an interspecific analysis was performed in STACKS (POPULATION module) to generate SNPs statistics between the two species. Specifically, we obtained LOD scores (likelihood odds ratio logarithm > 3), which estimates linkage disequilibrium between a SNP and the biological entities, and the Fisher's probability (P) of SNPs fixation index (Fst). Finally, the package "qqman" v. 0.1.4 (https://CRAN.Rproject.org/package=qqman) in the R software environment v. 3.4.1 (R Development Core Team, 2014) was used to construct a Manhattan plot using Fisher's P values to identify SNP alleles significantly associated with each species. In addition, SNPs identity was assessed using the BLAST algorithm in Genbank (https://www.ncbi.nlm.nih.gov/genbank/), using the genome of *Ictalurus punctatus* (Rafinesque, 1818) (Genbank accession number: LBML00000000) as a reference.

RESULTS

Traditional and geometric morphometrics. Repeatability of aligned coordinates ranged between 0.944 and 0.991. For centroid size, the value was 0.994 while for partial warps, the repeatability analysis returned values between 0.917 and 0.996. PCA of the landmark data showed that the first principal component, which explains 58% of the total variation, separates the body shape of *Pimelodus* into two large groups (Pg: *P. grosskopfii*; Py: *P. yuma*; Fig. 3). Euclidean distances between these groups were significant whether comparing females separately (PgF-PyF = 0.085, P = 0.000), males separately (PgM-PyM = 0.094, P = 0.000) or comparing different sexes of different species (PgF-PyM = 0.084, P

= 0.000; PgM-PyF = 0.093, P = 0.000). Allometric differences could not be size corrected due to differences in allometric slopes detected by the MANCOVA ($F_{42, 309.3}$ = 1.807, P = 0.003). Between sexes, allometric (PyF-PyM = 0.020, P = 0.044) and non-allometric (PyF-PyM = 0.018, P = 0.000; F14, 48 = 0.968, P = 0.499) differences were significant in *P. yuma*, while non-significant in *P. grosskopffi* (PgF-PgM = 0.012, P = 0.165).

The Simple Assignment analysis (Pg: 60/60, 100%; Py: 65/65, 100%) and Verified Cross-Classification (Pg: 60/60, 100%; Py: 65/65, 100%) confirmed that individuals separated by the first principal component in the PCA belong to the differentiated groups. That result demonstrates the existence of two distinct groups corresponding to the two species. That major difference does not result from sexual dimorphism.

Average body shape comparison of each group (Fig. 4) revealed allometric differences showing that the body of *P. grosskopfii* tends to be more streamlined and hydrodynamic than *P. yuma*, which seems to have a slightly taller and more robust body shape. In addition, within *P. yuma*, females (PyF) tend to be slightly taller than males (PyM), while in *P. grosskopfii* these differences were not significant.

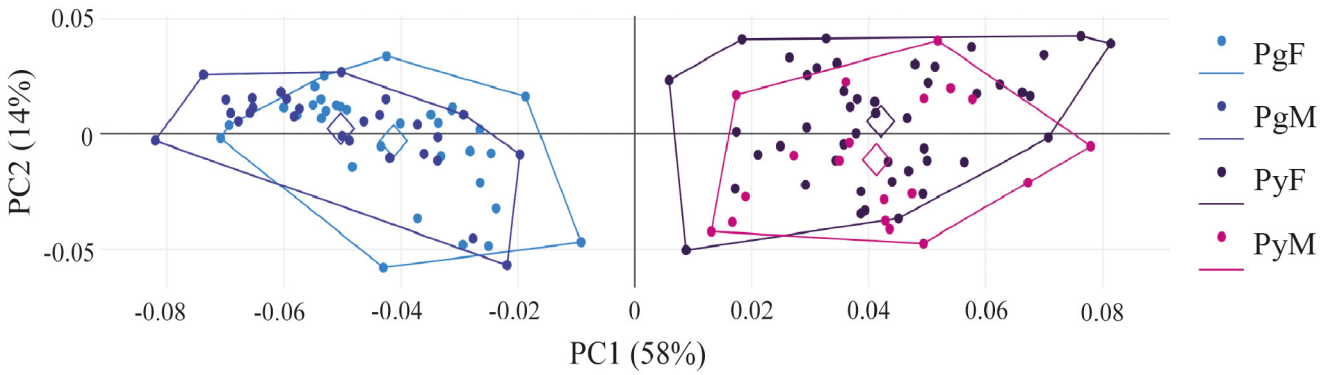

FIGURE 3 | Plot of the two first principal components (PC1, PC2) based on the body shape of females and males of *Pimelodus grosskopfii* (PgF, PgM) and *P. yuma* (PyF, PyM). Euclidean distances between species: PgF-PyF= 0.085, P = 0.000; PgM-PyM = 0.094, P = 0.000; PgF-PyM = 0.084, P = 0.000; PgM-PyF = 0.093, P = 0.000. Euclidean distances between sexes: PyF-PyM = 0.018, P = 0.000; PgF-PgM = 0.012, P = 0.165.

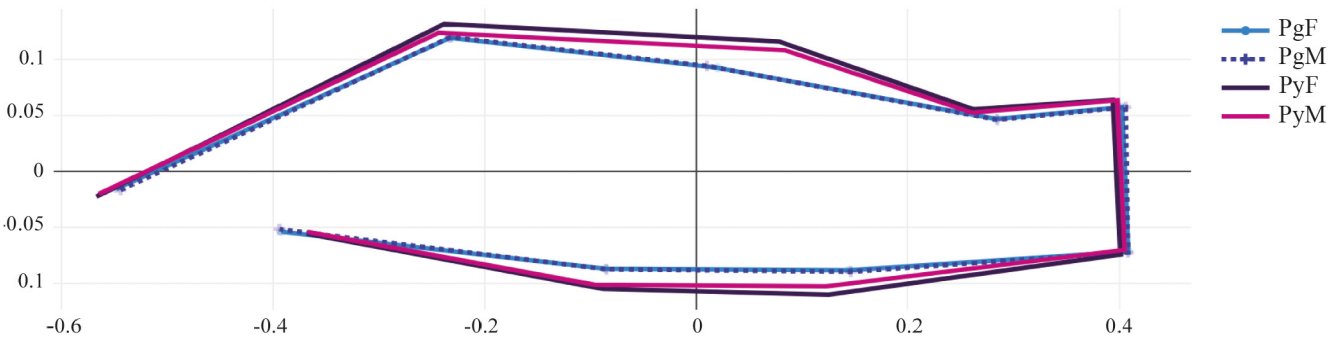

FIGURE 4 | Differences in body shape average of females and males of *Pimelodus grosskopfii* (PgF, PgM) and *P. yuma* (PyF, PyM) after the Generalized Procrustes analysis.

Regarding size, statistically significant differences were found between species ($F_{1, 122}$ = 163.632, P < 0.000), however, there were no significant effects between sexes ($F_{1, 122}$ = 0.361, P = 0.549) nor in the Species x Sex interaction ($F_{1, 121}$ = 2.564, P = 0.112). Specifically, *P. grosskopfii* males and females were larger than those of *P. yuma* (Fig. 5). Pairwise comparisons between PyF-PgF (P = 0.000), PyM-PgF (P = 0.000), PyF-PgM (P = 0.000), and PyM-PgM (P = 0.000), showed significant differences between the means of each group.

Thirty-four traditional measurements discriminated the two species (Fig. 6; Tab. 1), although only six contributed most greatly to the species discrimination: L1–L2: predorsal length, L1–L3: distance between the tip of the snout and the adipose-fin origin; L2–L3: distance between the dorsal-fin origin and adipose-fin origin; L3–L4: adipose fin length; L3–L8: distance between the adipose-fin origin and the pelvic-fin origin; L3–L9: distance between the adipose-fin origin and pectoral-fin origin.

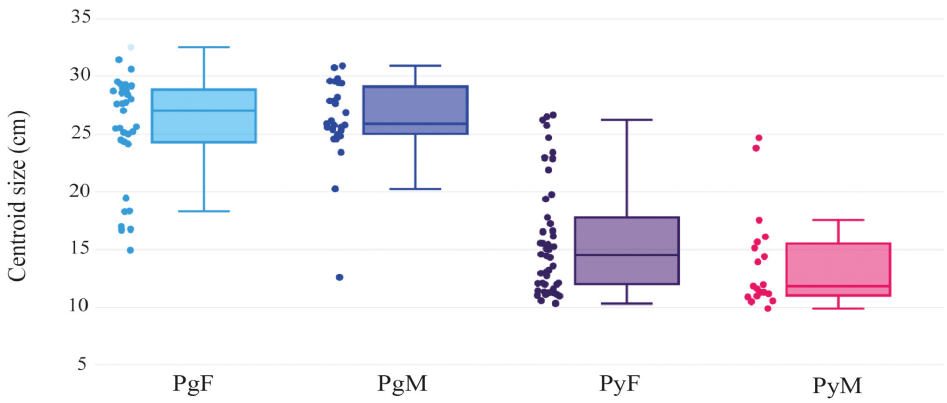

FIGURE 5 | Box and whisker plot of centroid sizes of females and males of *Pimelodus grosskopfii* (PgF, PgM) and *P. yuma* (PyF, PyM).

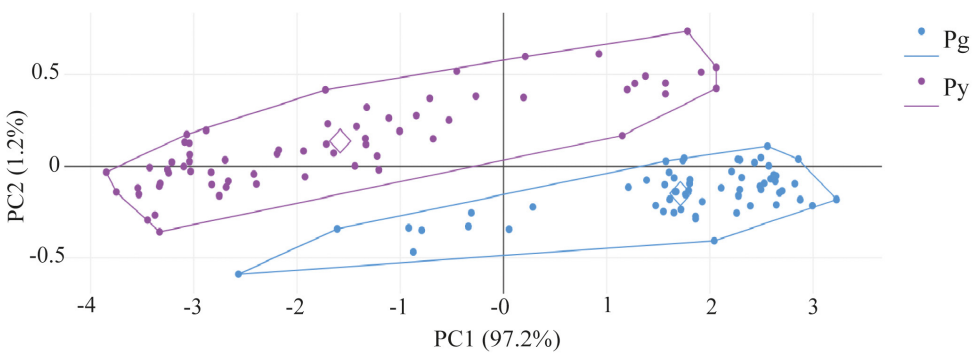

FIGURE 6 | Plot of the two first principal components (PC1: 97.2%, PC2: 1.2%) based on traditional measurements of *Pimelodus grosskopfii* (Pg) and *P. yuma* (Py). PC3 (0.6%) does not help to discriminate the species and may represent minor measurement error.

TABLE 1 | Principal components (PC) loading from traditional measurements.*Major contribution to the species discrimination.

Distance	Description	PC1 (97.2%)	PC2 (1.2%)
L1L2*	Tip of the snout to dorsal-fin origin (predorsal length)	0.16040	0.05001
L1L3*	Tip of the snout to adipose-fin origin	0.14125	0.16388
L1L4	Tip of the snout to adipose-fin insertion	0.16953	-0.03373
L1L7	Tip of the snout to anal-fin origin	0.17075	-0.02167
L1L8	Tip of the snout to pelvic-fin origin	0.16318	0.01443
L1L9	Tip of the snout to pectoral-fin origin	0.11388	0.15654
L2L3*	Dorsal-fin origin to adipose-fin origin	0.11880	0.31425
L2L4	Dorsal-fin origin to adipose-fin insertion	0.17469	-0.06047
L2L5	Dorsal-fin origin to origin of posterior most dorsal caudal-fin rays	0.17048	-0.03588
L2L6	Dorsal-fin origin to origin of posterior most ventral caudal-fin rays	0.16733	-0.02588
L2L7	Dorsal-fin origin to anal-fin origin	0.17360	0.04299
L2L8	Dorsal-fin origin to pelvic-fin origin	0.16538	0.22017
L2L9	Dorsal-fin origin to pectoral-fin origin	0.19313	0.08590
L3L4*	Adipose-fin origin to adipose-fin insertion (adipose fin length)	0.23945	-0.49314
L3L5	Adipose-fin origin to origin of posterior most dorsal caudal-fin rays	0.21055	-0.30881
L3L6	Adipose-fin origin to origin of posterior most ventral caudal-fin rays	0.19641	-0.20108
L3L7	Adipose-fin origin to anal-fin origin	0.18750	0.16543
L3L8*	Adipose-fin origin to pelvic-fin origin	0.12872	0.48576
L3L9*	Adipose-fin origin to pectoral-fin origin	0.15521	0.17530
L4L5	Adipose-fin insertion to origin of posterior most dorsal caudal-fin rays	0.15421	0.07022
L4L6	Adipose-fin insertion to origin of posterior most ventral caudal-fin rays	0.15252	0.12464
L4L7	Adipose-fin insertion to anal-fin origin	0.15941	0.16630
L4L8	Adipose-fin insertion to pelvic-fin origin	0.17674	-0.01526
L4L9	Adipose-fin insertion to pectoral-fin origin	0.18574	-0.07811
L5L6	Origin of posterior most dorsal caudal-fin rays to origin of posterior most ventral caudal-fin rays	0.16616	0.12736
L5L7	Origin of posterior most dorsal caudal-fin rays to anal-fin origin	0.15733	0.06610
L5L8	Origin of posterior most dorsal caudal-fin rays to pelvic-fin origin	0.17107	-0.01498
L5L9	Origin of posterior most dorsal caudal-fin rays to pectoral-fin origin	0.18035	-0.05928
L6L7	Origin of posterior most ventral caudal-fin rays to anal-fin origin	0.15079	-0.02532
L6L8	Origin of posterior most ventral caudal-fin rays to pelvic-fin origin	0.16782	-0.05708
L6L9	Origin of posterior most ventral caudal-fin rays to pectoral-fin origin	0.17791	-0.07206
L7L8	anal-fin origin to pelvic-fin origin	0.18782	-0.09084
L7L9	Anal-fin origin to pectoral-fin origin	0.19124	-0.08598
L8L9	Pelvic-fin origin to pectoral-fin origin	0.19374	-0.07538

Compared to *P. yuma*, *P. grosskopfii* was significantly longer in the L3–L4 measurement ($t_{111.18}$ = 24.77; P < 0.05), but had significantly shorter mean values for the measurements L1–L3 (t_{123} = -21.02; P < 0.05), L3-L9 (X^2_1= -59.89; P < 0.05), L1–L2 (W_1 = 705; P < 0.05), L2–L3 (t_{123} = -21.02; P < 0.05), and L3–L8 ($t_{110.12}$ = -19.31; P < 0.05) (Tab. 2). Additionally, in the ratios of each measurement to the length of the adipose fin, *P. grosskopfii* showed significantly lower values than *P. yuma* (Tab. 2) for L1–L3 ($t_{86.276}$= -18.20, P < 0.05), L3–L9 (t_{123}= -21.04; P < 0.05), L1–L2 ($t_{104.26}$= -23.49, P < 0.05), L2–L3 ($t_{110.96}$= -22.10; P < 0.05), and L3–L8 (W = 0.00, P < 0.05), implying that the length of the adipose fin base differs among these species. Despite the statistical differences, the intervals of these measurements overlapped in both groups, except for the ratio L3–L8/L3–L4, describing the distance between the origins of the pelvic and adipose fins divided by the length of the adipose fin base. This ratio decreased as the size increased in the total sample of *P. grosskopfii* (standard length: 12.2–31.2 cm), showing a negative relationship in a linear model that explains the 9.6% of the total variation (r = -0.310; r2 = 0.096; P = 0.016; Fig. 7). That same ratio varied isometrically in *P. yuma* (standard length: 9.5–25.4 cm) and remains independent of size (r = -0.110; r2 = 0.012; P = 0.384; Fig. 7).

Large individuals of these species were found to differ in body pigmentation. Specifically, larger individuals of *P. grosskopfii* possess separated and well-defined black spots distributed towards the anterior end or over the whole body. Smaller individuals of *P. grosskopfii* resemble some individuals of *P. yuma* by displaying spots with smaller diameters than those present in large individuals of *P. grosskopfii* group (Fig. 8).

TABLE 2 | Linear measurements of *Pimelodus grosskopfii* and *P. yuma* expressed as percentages of standard length or of the length of the adipose fin. SD = Standard deviation.

	Pimelodus grosskopfii				*Pimelodus yuma*			
	Mean	SD	Min	Max	Mean	SD	Min	Max
Percentage of standard length								
L1–L3	59.97	2.45	54.94	65.95	68.29	1.97	64.59	72.79
L3–L9	45.51	2.25	41.51	52.19	49.53	2.22	44.87	57.81
L1–L2	35.82	0.78	34.30	37.42	37.26	1.60	33.03	41.70
L2–L3	26.14	2.33	21.52	32.10	33.13	2.05	29.17	37.99
L3–L8	21.85	1.53	18.01	25.71	28.69	2.37	21.90	35.02
L3–L4	28.57	2.26	23.68	32.75	19.78	1.75	15.27	25.32
Proportion of the adipose fin								
L3–L9/L3–L4	1.61	0.19	1.31	2.00	2.53	0.29	1.90	3.32
L1–L2/L3–L4	1.26	0.11	1.08	1.48	1.90	0.19	1.46	2.41
L2–L3/L3–L4	0.93	0.15	0.68	1.29	1.69	0.23	1.15	2.30
L3–L8/L3–L4	0.77	0.09	0.56	0.97	1.46	0.27	1.10	2.01
L1–L3/L3–L4	0.39	0.08	0.29	0.63	0.83	0.50	0.48	1.19

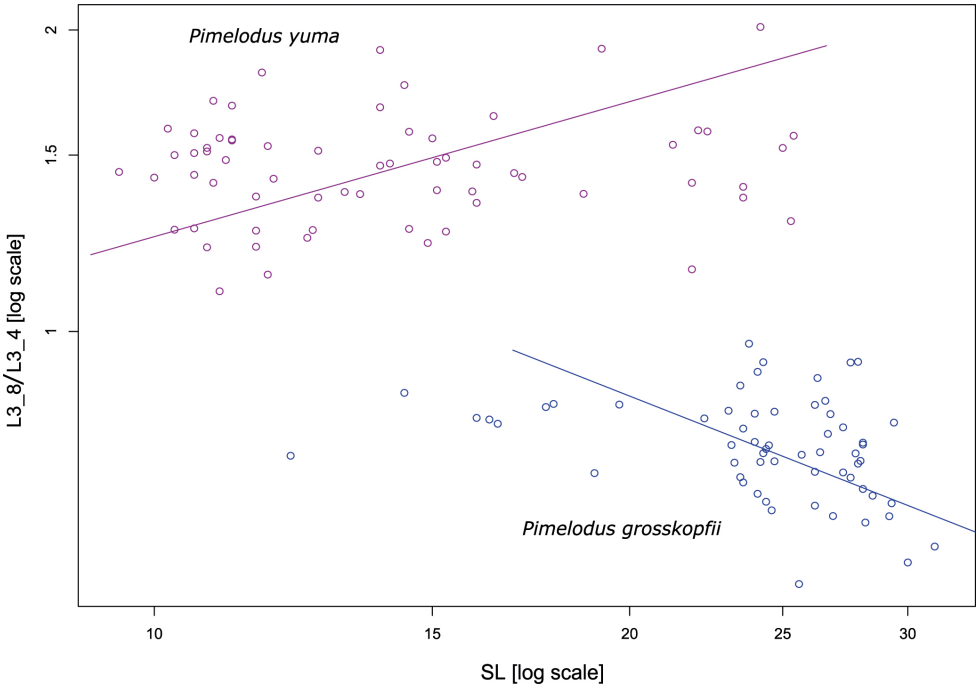

FIGURE 7 | Standardized major axis regression of the ratio L3–L8/L3–L4 on standard length for *Pimelodus grosskopfii* and *P. yuma*. L3–L8: distance between the adipose-fin origin and the pelvic-fin insertion. L3–L4: length of the adipose fin.

FIGURE 8 | Body pigmentation of *Pimelodus grosskopfii* (**A**) and *P. yuma* (**B**). Scale bars = 1 cm.

Phylogenetic analyses. After sequence edition, we obtained an alignment 489 bp in length of the *cox1* gene (GenBank accession numbers: ON596020 – ON596098; ON596100 – ON596145). Translation into amino acids revealed no indels or stop codons, showing that the alignment corresponds to functional *cox1* gene sequences. A total of 17 haplotypes of *P. grosskopffi* made up two haplogroups that clustered within the reference *P. grosskopfii* clade (posterior probability = 1), while 11 haplotypes of *P. yuma* females made up two haplogroups that clustered with reference *P. yuma* (posterior probability = 1), showing a 100% concordance between with morphometric assignation of individuals to species (Fig. 9).

Additionally, the Kimura 2 parameter genetic distance was high between *P. grosskopfii* and *P. yuma* (0.113), and relatively small between haplogroups (*P. grosskopfii* haplogroups: 0.010; *P. yuma* haplogroups: 0.007) and within species (*P. grosskopfii*: 0.008; *P. yuma*: 0.005). Based on the differences in the *cox1* sequences, two primer pairs were designed for *P. grosskopfii* (Pgrocox1F: 5´-CCAAATTTATAACGTCATCGTA-3´; Pgrocox1R: 5´-GAGGCAAGGAGGAGGAGGAACG-3´, product length: 192pb) and *P. yuma* (Pyumcox1F: 5´-CCAAATTTACAACGTTATCGTT; Pyumcox1R: 5´-GAGGCAAGCAGGAGAAGGAATG-3´, product length: 192pb).

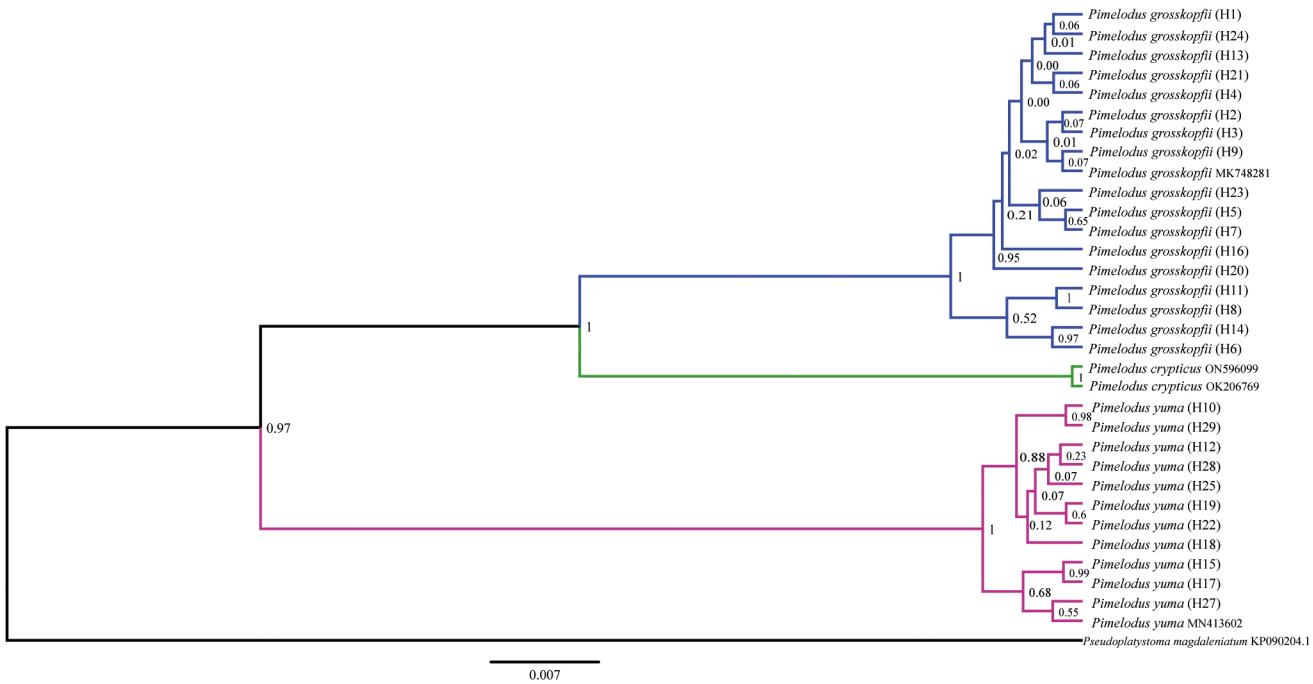

FIGURE 9 | Bayesian phylogenetic tree based on partial *cox1* gene sequences, showing the phylogenetic relationships of individuals analysed in this study with the barcode-confirmed species *Pimelodus grosskopfii*, *P. crypticus*, and *P. yuma*.

Identification of diagnostic SNPs. The best constraint settings found by RADproc analysis were *-M* = 2 and *-m* = 3, and the effective coverage per sample generated by STACKS analyses showed a mean = 19.1x, stdev = 4.0x, min = 12.5x, and max = 26.7x. A total of 11,336 sites were retained corresponding to 120 loci, of which 51 unlinked SNPs (no more than one per locus) were detected after verifying all quality criteria. STRUCTURE results using the 51 SNPs corroborated the barcode analysis, showing K = 2 as the most likely number of genetic groups (LnP[data] = -489.95; *P. grosskopfii*: 24 individuals; *P yuma*: 10 individuals, coancestry level > 98%; Fig. 10).

A total of eight SNPs (loci 1997, 5141, 5961, 7493, 9294, 12198, 12611, and 32968) displayed species association, with LOD scores > 3. However, according to the Manhattan plot results, only five (1997, 5141, 5961, 9294, and 12198) were differentially associated with each species (Fig. 11). As seen in Tab. 3, three of these loci have reciprocally exclusive alleles: 1997 [*P. yuma*: (G); *P. grosskopfii*: (C)], 5961 [*P. yuma*: (C); *P. grosskopfii*: (G)] and 12198 [*P. yuma*: (T); *P. grosskopfii*: (C)]. The two remaining loci showed no reciprocally exclusive alleles but had high frequency or fixation for one of the two species: 5141 [*P. yuma*: (T); *P. grosskopfii*: (C)], 9294 [*P. yuma*: (C); *P. grosskopfii*: (A)].

FIGURE 10 | STRUCTURE results based on unlinked SNP analysis for *Pimelodus grosskopfii* and *P. yuma*.

TABLE 3 | Characterization of putative species-specific SNPs markers for *Pimelodus grosskopfii* (Pg) and *P. yuma* (Py). The identity and genomic location of the SNPs were conducted using the genome of *Ictalurus punctatus* (assembly IpCoco_1.2) as a reference, due to identity and phylogenetic proximity as identified by BLAST. E: species; Aa: coded amino acid; ST: Type of substitution (NS: not synonymous; S: Synonymous); IFG: interspecific genotypic frequency; IAF: interspecific allelic frequency.

Locus	Putative gene	E	Genotypes	Aa	ST	IFG	IAF
1997	Sarcoglycan zeta/Chr 29 (NC_030444.1)	Pg	C/C	His	NS	1	C=1/G=0
		Py	G/G	Asp	NS	1	C=0/G=1
5141	Claudin-4-like/Chr 20 (NC_030435.1)	Pg	C/C	Phe	S	1	C=1/T=0
		Py	C/T; T/T	Phe	S	0.4; 0.6	C=0.2/T=0.8
5961	Anonymous	Pg	G/G	-	-	1	G=1/C=0
		Py	C/C	-	-	1	G=0/C=1
9294	WNK proteína quinasa deficiente en lisina 1/Chr 19 (NC_030434.1)	Pg	A/A; A/C; C/C	Met; Leu	NS	0.833; 0.125; 0.042	A=0.9/C=0.1
		Py	C/C	Leu	NS	1	A=0/C=1
12198	Anonymous	Pg	C/C	-	-	1	C=1/T=0
		Py	T/T	-	-	1	C=0/T=1

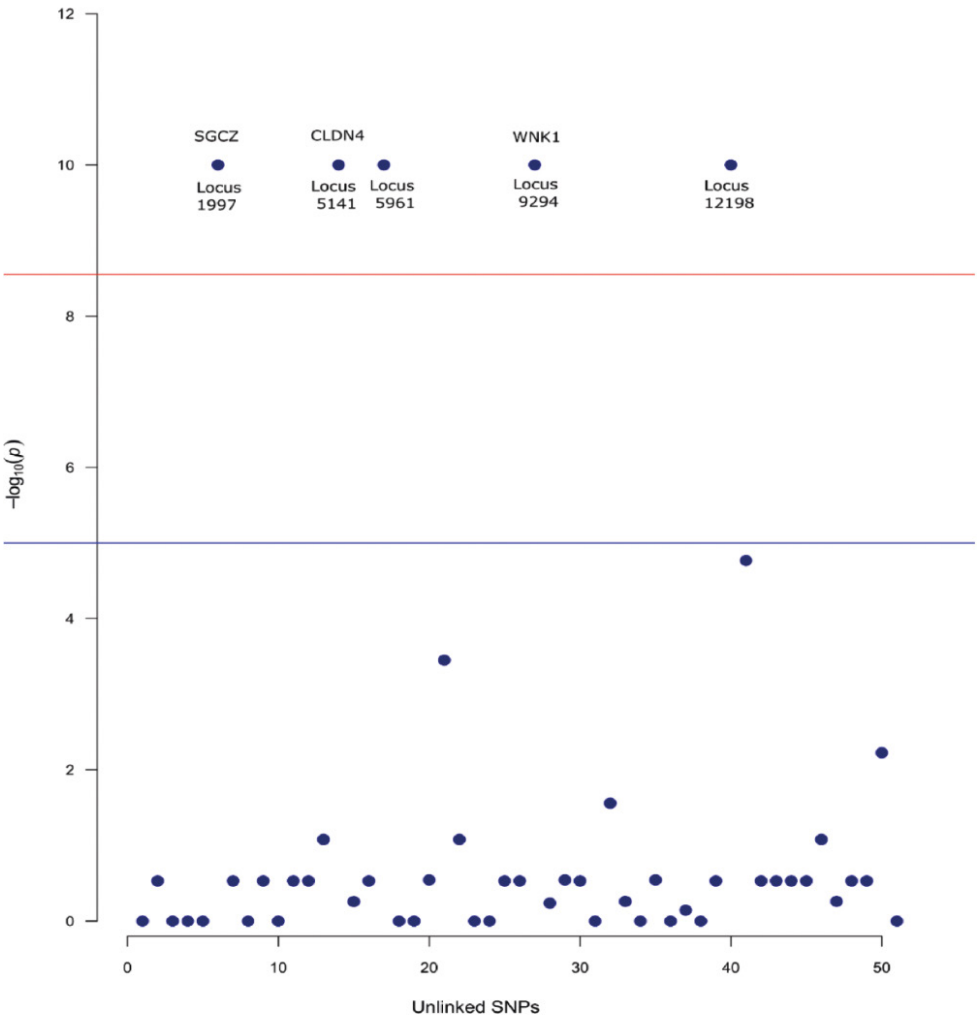

FIGURE 11 | Manhattan plot depicting SNP loci that can differentiate *Pimelodus grosskopfii* and *P. yuma*. (p): P value for each of the 51 polymorphisms (unlinked-SNPs) tested by Fisher's test. The blue and red lines show significance threshold at $P < 1\times10^{-5}$ and $P < 5\times10^{-9}$, respectively.

BLAST analysis against the genome of *Ictalurus punctatus* showed that locus 1997 corresponded to an exonic region of the zeta-sarcoglycan (SGCZ) gene, (involved in muscle development). Locus 5141 fell within the claudin 4 gene (CLDN4), which controls the passage of solute/water in the gills. Locus 9294 corresponded with WNK1-WNK1 lysine-deficient protein kinase, which controls blood pressure and regulates sodium/potassium transport in the kidney). The other two species-specific loci (5961 and 12198) corresponded to anonymous genomic regions. While the substitution at locus 5141 (Claudin-4-like/Chr 20 gene) is synonymous and thus selectively neutral, SNPs at loci 1997 (SGCZ gene) and 9294 (WNK1 gene) produced non-synonymous mutations (Tab. 3).

Using the SNP in the 3`end of the forward primer, three primer pairs were designed for amplifying the diagnostic loci in *P. grosskopfii*. These are 1997 (Pg1997F: 5`- AACTCCCCCACTCCTGCATTC-3`; Pg1997R: 5`-TCTCCGACGCGGACTCTG-3`, product length: 68pb), 5961 (Pg5961F: 5`- CCTTCCCATGGTGCCCTGGGG-3`; Pg5961R: 5`-GGAACCAACGCTCCTGAGACC-3`; product length: 84pb) and 12198 (Pg12198F: 5`-TGCACCTGCCTC; Pg12198R: 5`-TGAACCACTCCATCTAGGACA; product length: 78pb). These primers may amplify the same loci in *P. yuma* replacing the corresponding SNP in the 3`end of the forward primer. In contrast to the specific primers designed for the loci 5961 and 12198, the primers designed for amplifying the locus 1997 may show potential amplifications with other fish genera such as *Ictalurus punctatus*, *Tachysurus sinensis* Lacepède, 1803, *Pygocentrus nattereri* Kner, 1858, *Pangasianodon hypophthalmus* (Sauvage, 1878), *Astyanax mexicanus* (De Filippi, 1853), *Electrophorus electricus* (Linnaeus, 1766), *Carassius auratus* (Linnaeus, 1758), and *Plectropomus leopardus* (Lacepède, 1802), as revealed by the BLAST and global alignment algorithm to screen non-specific amplifications of primer pairs against a user-selected database (Ye *et al*., 2012).

DISCUSSION

This study conducted an integrative analysis combining traditional and geometric morphometrics, phylogenetic analysis using *cox1* gene sequences, and identification of diagnostic SNP markers to improve the discrimination of the catfish species *Pimelodus grosskopfii* and *P. yuma*. Our results show that traditional and geometric morphometrics can reliably discriminate these congeners by body shape, as could phylogenetic analysis of information contained in *cox1* sequence data. For the first time, genomic SNP markers with exclusive alleles were found to also discriminate these species.

Traditional, geometric morphometrics and phylogenetic analyses. Principal components analyses based on geometric and traditional data revealed the existence of two groups with differences in body shape. Assignment analyses classified all individuals to one of these groups with high confidence. These results were corroborated by *cox1* gene sequence analyses, which accurately clustered the haplotypes belonging to each morphological group with those of known sequences of *P. grosskopfii* and *P. yuma*. The phylogenetic approach also corroborates that the species described by Villa-Navarro *et al*., (2017) in the Magdalena-Cauca basin represent monophyletic groups clearly distinguishable by *cox1* sequences (Martínez *et al*., 2022), as evidenced by the high posterior probability values that supports the observed clustering. Based on the divergence of *cox1* sequences between species, two pairs of primers were designed to discriminate them, although its experimental evaluation and consequent usefulness remains to be explored.

Although two haplogroups were found in each species, the Kimura 2 parameter genetic distances between those haplogroups are less than 1%, suggesting that they do not represent cryptic species (Ward *et al*., 2009). However, further integrative studies would be required to fully test a hypothesis of further unrecognized diversity in this clade.

The observed differences in average body shape of females and males established that *P. grosskopfii* has a more streamlined body, and hence may be more hydrodynamic than *P. yuma*. These results accord with the different environments that these species inhabit. *Pimelodus yuma* is restricted to the lower sector of the Cauca River (Villa-Navarro *et al*., 2017) and experiences relatively stable hydrodynamic conditions, while *P. grosskopfii* migrates to the upper sector (Restrepo-Escobar *et al*., 2021), and experiences many different flow regimes. It was previously reported that differences between lotic and lentic habitats can induce body shape differences in this species (Hincapié-Cruz, Márquez, 2021).

Exploring intrinsic sources of phenotypic variation, this study detected no sexual dimorphism in body shape or size in *P. grosskopfii*, which concords with Cala (1997), though Valbuena-Villarreal *et al*. (2010) suggested dimorphism in size for this species. In contrast, we detected differences in body shape between sexes of *P. yuma*, especially in body height between the origin of the dorsal fin and the origin of the adipose fin and at the origin of the anal fin. Further studies should explore these results in individuals with similar states of gonadal development (Vazzoler, 1996), since reproductive maturity and gravidity may affect the body shape of the individuals analysed.

Previous traditional morphometric analysis suggested that the size of the adipose fin and the predorsal distance are the measurements that best differentiate *P. grosskopfii* from *P. yuma* (Villa-Navarro *et al*., 2017). However, we found the range of these variables to overlap in the two species, prompting a search for additional traits that allow discrimination. Herein we examined four measurements related to the length of the adipose fin, which differ from those reported by Villa-Navarro *et al*. (2017). The ranges of three of these measurements also overlap among the species, but the ranges of the ratio L3–L8/L3–L4 do not. This ratio juxtaposes the distance between the adipose-fin origin and pelvic-fin origin with the length of the adipose-fin base and provides a measurement that allows easier differentiation of these species. Likewise, the differences in the allometric trajectories of *P. grosskopfii* and *P. yuma* represent an additional point of discriminating both species; and their visualization in the same plot (Fig. 7) provides a reference for the diagnosis of those species.

Additionally, this study found variations in body pigmentation patterns in both species. Although all the large-sized individuals of *P. grosskopfii* showed dark spots on their bodies, smaller individuals showed smaller spots like those seen in some *P. yuma* specimens, which shows that the skin pigmentation is a variable trait and its validity as a distinctive characteristic is limited. Intraspecific variations in the skin coloration pattern have been described for species of *Pseudoplatystoma* Bleeker, 1862 (Buitrago-Suárez, Burr, 2007; Scarabotti *et al*., 2020), *Pseudopimelodus* Bleeker, 1858 (Restrepo-Gómez *et al*., 2020), *Pagrus pagrus* (Linnaeus, 1758) (Van Der Salm *et al*., 2004), *Trichogaster pectoralis* Regan, 1910 (Ninwichian *et al*., 2018), among others (Sugimoto, 2002).

Identification of diagnostic SNPs. This study identified for first time a set of diagnostic SNPs that can be used to discriminate *P. grosskopfii* from *P. yuma*, which were previously separated genetically with only mitochondrial *cox1* sequences. Five loci exhibited strong differential association with each species, and three of these loci had exclusive alleles in homozygous state in both species. Therefore, 2.5% of the total 120 SNPs perfectly separate these species. A study of four tilapia species found a slightly lower detection efficiency of 1.8% in a panel of 1371 SNPs obtained from partial

genome sequencing (ddRADseqs) (Syaifudin *et al*., 2019). Although SNPs allowed the differentiation by species, we recommended a further validation study using more samples to assess the efficacy of these markers in discriminating both species via PCR-based methods. For this proposal, the primers designed for the loci 5961 and 12198 are highly recommended, whereas the primers for the locus 1997 may not be specific, showing potential in silico amplifications with other fish genera. Since the SNP is in the 3`end of the forward primer in all loci, stringent PCR conditions are required to avoid non-specific amplifications. Due to the forward primer for the locus 12198 is short (12 mer in length), its length may be increased using adaptors attached on its 5`end such as those described by Blacket *et al*. (2012) or the M13 tail.

Whether the differentially expressed genes influence the fitness and distribution of these species is currently unknown. Given the wider distribution of *P. grosskopfii*, it is expected that this species has a better ability to face different environments, suggesting that a SNP within a gene related to the development of skeletal and cardiac muscle could be associated with its distribution. Scott, Johnston (2012) showed that embryonic temperature in zebrafish can have dramatic and persistent effects on acclimatization ability at multiple levels of biological organization. Performance differences following temperature acclimatization from cold to hot were partially explained by fiber type composition in swimming muscles. In addition, differences were observed in the expression of genes involved in energy metabolism, angiogenesis, cell stress, contraction and muscle remodelling, and apoptosis. Although the Claudin-4 gene has a pivotal role in salinity adaptation in the flounder species *Paralichthys lethostigma* Jordan & Gilbert, 1884 (Tipsmark *et al*., 2008), it does not seem to provide differential tolerance to physicochemical changes (atmospheric pressure, dissolved oxygen, temperature, total solutes, and pH) in *P. grosskopfii* and *P. yuma*, as synonymous mutations were found in both species. However, since the effect of genetic drift may also explain our results, these hypotheses must be assessed in more individuals and with suitable experimental designs that allow to understand the role of these genetic polymorphisms in the physiology of these species.

In line with the above-mentioned statements, the SNP with non-synonymous mutations 9294 (WNK1) exhibited high genotypic frequencies for the "AA" genotype in *P. grosskopfii* from upper and middle sections of the Cauca and Magdalena rivers (AA = 0.833; AC = 0.125; CC = 0.042), whereas the "CC" genotypes were found exclusively in the lower section of the Cauca River. Although samples from the lower section of the Magdalena River remains to be examined and more studies are needed, these genotypic frequencies seem to be a marker for the upper/middle (Cauca River: AA; Magdalena River: AA > AC) and lower sector (Cauca River: CC) environments of the Magdalena and Cauca rivers. This outcome differs from that observed in *P. yuma*, where the genotype "CC" found in all assessed individuals (n = 10) was present in the sectors evaluated of the Cauca and Magdalena rivers.

In conclusion, this study demonstrates that four methodological approaches can discriminate the congeners *P. grosskopfii* and *P. yuma*: traditional and geometric morphometrics, phylogenetic analysis of the partial sequence of the *cox1* gene and SNPs. These approaches, which can be used separately or in combination by researchers with differing areas of expertise, support the recognition of these species as valid and can help to assign individuals from wild and captive populations to the correct species. That in turn, provides a crucial step for the preservation of these animals and proper management of the fishery that depends upon them.

ACKNOWLEDGMENTS

This work was funded by Empresas Públicas de Medellín and the Universidad Nacional de Colombia, Sede Medellín through the scientific agreement "Variabilidad genética de un banco de peces de los sectores medio y bajo del río Cauca - CT–2019–000661", Universidad Nacional de Colombia, Sede Medellín, Colciencias, Institución Universitaria Colegio Mayor de Antioquia "Delimitación de Unidades Evolutivas Significativas para la conservación de especies de peces del género *Pimelodus* en los Andes colombianos: una aproximación genómico-poblacional y filogenómica para la cuenca Magdalena-Cauca - Hermes 40096, FCS–2017, and Institución Universitaria Colegio Mayor de Antioquia - Universidad Nacional de Colombia sede Medellín, "Genética de la conservación de especies de peces Trasandinas colombianas del género *Pimelodus*: una aproximación genómico-poblacional para la cuenca Magdalena-Cauca - FCSA20". The authors thank Brian Sidlauskas and the anonymous reviewers for their comments that improved the final version of this article.

REFERENCES

- **Arcila D, Vari RP, Menezes NA.** Revision of the Neotropical genus *Acrobrycon* (Ostariophysi: Characiformes: Characidae) with description of two new species. Copeia. 2013; 2013(4):604–11. https://doi.org/10.1643/CI-13-009
- **Becker RA, Sales NG, Santos GM, Santos GB, Carvalho DC.** DNA barcoding and morphological identification of neotropical ichthyoplankton from the Upper Paraná and São Francisco. J Fish Biol. 2015; 87(1):159–68. https://doi.org/10.1111/jfb.12707
- **Bingpeng X, Heshan L, Zhilan Z, Chunguang W, Yanguo W, Jianjun W.** DNA barcoding for identification of fish species in the Taiwan Strait. PLoS ONE. 2018; 13(6):e0198109. https://doi.org/10.1371/journal.pone.0198109
- **Blacket MJ, Robin C, Good RT, Lee SF, Miller AD.** Universal primers for fluorescent labelling of PCR fragments-an efficient and cost-effective approach to genotyping by fluorescence. Mol Ecol Resour. 2012; 12(3):456–63. https://doi.org/10.1111/j.1755-0998.2011.03104.x
- **Bookstein F.** Morphometric tools for landmark data: Geometry and biology. Cambridge: Cambridge University Press; 1992. https://doi.org/10.1017/CBO9780511573064
- **Bouckaert R, Vaughan TG, Barido-Sottani J, Duchêne S, Fourment M, Gavryushkina A *et al*.** BEAST 2.5: An advanced software platform for Bayesian evolutionary analysis. PLoS Comput Biol. 2019; 15(4): e1006650. https://doi.org/10.1371/journal.pcbi.1006650
- **Buitrago-Suárez UA, Burr BM.** Taxonomy of the catfish genus *Pseudoplatystoma* Bleeker (Siluriformes: Pimelodidae) with recognition of eight species. Zootaxa. 2007; 1512(1):1–38. https://doi.org/10.11646/zootaxa.1512.1.1
- **Cala-Cala P.** Medio ambiente y diversidad de los peces de agua dulce de Colombia. Bogotá: Academia Colombiana de Ciencias Exactas, Físicas y Naturales; 2019. Available from: https://repositorio.accefyn.org.co/handle/001/115
- **Cala P.** Espermatogénesis y ciclo anual reproductivo del capaz, *Pimelodus grosskopfii* (pisces: Pimelodidae), en el alto río Magdalena, Colombia. Caldasia. 1997; 19(1–2):45–53.
- **Catchen J, Hohenlohe PA, Bassham S, Amores A, Cresko WA.** Stacks: An analysis tool set for population genomics. Mol Ecol. 2013; 22(11):3124–40. https://doi.org/10.1111/mec.12354
- **Darriba D, Taboada GL, Doallo R, Posada D.** JModelTest 2: More models, new heuristics and parallel computing. Nat Methods. 2012; 9(8):772. https://doi.org/10.1038/nmeth.2109

- **Díaz J, Villanova GV, Brancolini F, Pazo F Del, Posner VM, Grimberg A *et al*.** First DNA barcode reference library for the identification of South American freshwater fish from the lower Paraná River. PLoS ONE. 2016; 11(7): e0157419. https://doi.org/10.1371/journal.pone.0157419
- **Dujardin S, Dujardin JP.** Geometric morphometrics in the cloud. Infect Genet Evol. 2019; 70:189–96. https://doi.org/10.1016/j.meegid.2019.02.018
- **Duranton M, Allal F, Fraïsse C, Bierne N, Bonhomme F, Gagnaire PA.** The origin and remolding of genomic islands of differentiation in the European sea bass. Nat Commun. 2018; 9(1):2518. https://doi.org/10.1038/s41467-018-04963-6
- **Ferrer J, Malabarba LR.** Taxonomic review of the genus *Trichomycterus* Valenciennes (Siluriformes: Trichomycteridae) from the laguna dos Patos system, Southern Brazil. Neotrop Ichthyol. 2013; 11(2):217–46. https://doi.org/10.1590/S1679-62252013000200001
- **Frantine-Silva W, Sofia SH, Orsi ML, Almeida FS.** DNA barcoding of freshwater ichthyoplankton in the Neotropics as a tool for ecological monitoring. Mol Ecol Resour. 2015; 15(5):1226–37. https://doi.org/10.1111/1755-0998.12385
- **Fricke R, Eschmeyer WN, Fong JD.** Eschmeyer's catalog of fishes: species by family/subfamily [Internet]. San Francisco: California Academy of Science; 2022a. Available from: http://researcharchive.calacademy.org/research/ichthyology/catalog/SpeciesByFamily.asp.
- **Fricke R, Eschmeyer WN, Van der Laan R.** Eschmeyer's catalog of fishes: genera, species, references [Internet]. San Francisco: California Academy of Science; 2022b. Available from: http://researcharchive.calacademy.org/research/ichthyology/catalog/fishcatmain.asp
- **Garavello JC, Ramirez JL, de Oliveira AK, Britski HA, Birindelli JLO, Galetti PM.** Integrative taxonomy reveals a new species of Neotropical headstanding fish in genus *Schizodon* (Characiformes: Anostomidae). Neotrop Ichthyol. 2021; 19(4):e210016. https://doi.org/10.1590/1982-0224-2021-0016
- **García-Alzate CA, Ruiz-C RI, Román-Valencia C, González MI, Lopera DX.** Morfología de las especies de *Hyphessobrycon* (Characiformes: Characidae), grupo *heterorhabdus*, en Colombia. Rev Biol Trop. 2011; 59(2):709–25. https://doi.org/10.15517/rbt.v0i0.3134
- **Goodall C.** Procrustes methods in the statistical analysis of shape. J Roy Stat Soc Ser B Met. 1991; 53(2):285–321. https://doi.org/10.1111/j.2517-6161.1991.tb01825.x
- **Guindon S, Gascuel O.** A simple, fast, and accurate algorithm to estimate large phylogenies by maximum likelihood. Syst Biol. 2003; 52(5):696–704. https://doi.org/10.1080/10635150390235520
- **Gupta D, Dwivedi AK, Tripathi M.** Taxonomic validation of five fish species of subfamily Barbinae from the Ganga River system of northern India using traditional and truss analyses. PLoS ONE. 2018; 13(10):e0206031. https://doi.org/10.1371/journal.pone.0206031
- **Hall TA.** BioEdit: a user-friendly biological sequence alignment editor and analysis program for Windows 95/98/NT. Nucl Acid S. 1999; 41:95–98.
- **Hebert PDN, Cywinska A, Ball SL, DeWaard JR.** Biological identifications through DNA barcodes. Proc R Soc B Biol Sci. 2003; 270(1512):313–21. https://doi.org/10.1098/rspb.2002.2218
- **Herler J, Kerschbaumer M, Mitteroecker P, Postl L, Sturmbauer C.** Sexual dimorphism and population divergence in the Lake Tanganyika cichlid fish genus *Tropheus*. Front Zool. 2010; 7(4):1–10. https://doi.org/10.1186/1742-9994-7-4
- **Heller P, Casaletto J, Ruiz G, Geller J.** A database of metazoan cytochrome c oxidase subunit I gene sequences derived from GenBank with CO-ARBitrator. Sci Data. 2018; 5:1–07. https://doi.org/10.1038/sdata.2018.156
- **Hernández-Barrero S, Barreto-Reyes CG, Valderrama-Barco M.** Presión de uso del recurso íctico por la pesca artesanal en la cuenca del río Magdalena, Colombia. In: Jiménez-Segura L, Lasso CA, editors. XIX Peces de la cuenca del río Magdalena, Colombia: diversidad, conservación y uso sostenible. Bogotá: Editorial Recursos Hidrobiológicos y Pesqueros Continentales de Colombia. Instituto de Investigación de Recursos Biológicos Alexander von Humboldt; 2020; p.369–87. https://doi.org/10.21068/a2020rrhhxix

- **Hincapié-Cruz JP, Márquez EJ.** Variación fenotípica de los peces *Curimata mivartii* (Characiformes: Curimatidae) y *Pimelodus grosskopfii* (Siluriformes: Pimelodidae) en hábitats lóticos y lénticos. Rev Biol Trop. 2021; 69(2):434–44. https://doi.org/10.15517/rbt.v69i2.41708
- **Hubert N, Hanner R, Holm E, Mandrak NE, Taylor E, Burridge M *et al*.** Identifying Canadian freshwater fishes through DNA barcodes. PLoS ONE. 2008; 3(6):e2490. https://doi.org/10.1371/journal.pone.0002490
- **Ivanova NV, Zemlak TS, Hanner RH, Hebert PDN.** Universal primer cocktails for fish DNA barcoding. Mol Ecol Notes. 2007; 7(4):544–48. https://doi.org/10.1111/j.1471-8286.2007.01748.x
- **Jiménez-Segura L, Herrera-Pérez J, Valencia- Rodríguez D, Castaño-Tenorio I, López-Casas S, Ríos MI *et al*.** Ecología e historias de vida de los peces de la cuenca del río Magdalena, Colombia: In: Jiménez-Segura L, Lasso CA, editors. XIX Peces de la cuenca del río Magdalena, Colombia: diversidad, conservación y uso sostenible. Bogotá; Colombia: Editorial Recursos Hidrobiológicos y Pesqueros Continentales de Colombia. Instituto de Investigación de Recursos Biológicos Alexander von Humboldt; 2020; p.159–203. https://doi.org/10.21068/a2020rrhhxix
- **Joya CD, Landínez-García RM, Márquez EJ.** Development of microsatellite loci and population genetics of the catfish *Pimelodus yuma* (Siluriformes: Pimelodidae). Neotrop Ichthyol. 2021; 19(1):e200114. https://doi.org/10.1590/1982-0224-2020-0114
- **Kocovsky PM, Sullivan TJ, Knight CT, Stepien CA.** Genetic and morphometric differences demonstrate fine-scale population substructure of the yellow perch *Perca flavescens*: Need for redefined management units. J Fish Biol. 2013; 82(6):2015–30. https://doi.org/10.1111/jfb.12129
- **Kopelman NM, Mayzel J, Jakobsson M, Rosenberg NA, Mayrose I.** Clumpak: a program for identifying clustering modes and packaging population structure inferences across K. Mol Ecol Resour. 2015; 15(5):1179–91. https://doi.org/10.1111/1755-0998.12387
- **Guimarães-Costa AJ, Machado FS, Oliveira RRS, Silva-Costa V, Andrade MC, Giarrizzo T *et al*.** Fish diversity of the largest deltaic formation in the Americas - a description of the fish fauna of the Parnaíba Delta using DNA Barcoding. Sci Rep. 2019; 9(1):1–08. https://doi.org/10.1038/s41598-019-43930-z
- **Lasso CA, Agudelo E, Córdoba L, Jiménez-Segura F, Ramírez-Gil H, Morales-Betancourt M *et al*.** I. Catálogo de los recursos pesqueros continentales de Colombia. Serie Editorial Recursos Hidrobiológicos y Pesqueros Continentales de Colombia. Instituto de Investigación de Recursos Biológicos Alexander von Humboldt. Bogotá: 2011.
- **Li YL, Liu JX.** StructureSelector: A web-based software to select and visualize the optimal number of clusters using multiple methods. Mol Ecol Resour. 2018; 18(1):176–77. https://doi.org/10.1111/1755-0998.12719
- **Londoño-Burbano A, Román-Valencia C, Taphorn DC.** Taxonomic review of Colombian *Parodon* (Characiformes: Parodontidae), with descriptions of three new species. Neotrop Ichthyol. 2011; 9(4):709–30. https://doi.org/10.1590/S1679-62252011000400003
- **Maderbacher M, Bauer C, Herler J, Postl L, Makasa L, Sturmbauer C.** Assessment of traditional versus geometric morphometrics for discriminating populations of the *Tropheus moorii* species complex (Teleostei: Cichlidae), a Lake Tanganyika model for allopatric speciation. J Zool Syst Evol Res. 2008; 46(2):153–61. https://doi.org/10.1111/j.1439-0469.2007.00447.x
- **Marcus L.** Traditional Morphometrics. In: Rohlf FJ, Bookstein FL, editors. Proceedings of the Michigan morphometrics workshop. University of Michigan, Museum of Zoology; 1990. p.77–123.
- **Martínez JG, Rangel-Medrano JD, Yepes-Acevedo AJ, Restrepo-Escobar N, Márquez EJ.** Species limits and introgression in *Pimelodus* from the Magdalena-Cauca River basin. Mol Phylogenet Evol. 2022; 173:107517. https://doi.org/10.1016/j.ympev.2022.107517
- **Martin SH, Jiggins CD.** Interpreting the genomic landscape of introgression. Curr Opin Genet Dev. 2017; 47:69–74. https://doi.org/10.1016/j.gde.2017.08.007

- **Nelson J, Grande T, Wilson M.** Fishes of the world. New Jersey: John Wiley & Sons; 2016.
- **Ninwichian P, Phuwan N, Jakpim K, Sae-Lim P.** Effects of tank color on the growth, stress responses, and skin color of snakeskin gourami (*Trichogaster pectoralis*). Aquacult Int. 2018; 26(2):659–72. https://doi.org/10.1007/s10499-018-0242-6
- **Pinto KS, Pires THS, Stefanelli-Silva G, Barros BS, Borghezan EA, Zuanon J.** Does soil color affect fish evolution? Differences in color change rate between lineages of the sailfin tetra. Neotrop Ichthyol. 2020; 18(2):e190093. https://doi.org/10.1590/1982-0224-2019-0093
- **Pritchard JK, Stephens M, Donnelly P.** Inference of population structure using multilocus genotype data. Genetics. 2000; 155:945–59.
- **Ravindran NP, Bentzen P, Bradbury IR, Beiko RG.** RADProc: A computationally efficient de novo locus assembler for population studies using RADseq data. Mol Ecol Resour. 2019; 19(1):272–82. https://doi.org/10.1111/1755-0998.12954
- **R Development Core Team.** R: A language and environmental for statistical computing. Vienna, Austria: R Foundation for Statistical Computing; 2013. Available from: https://www.r-project.org/
- **R Development Core Team.** R: A language and environmental for statistical computing. Vienna, Austria: R Foundation for Statistical Computing; 2014. Available from: https://www.r-project.org/
- **Rambaut A, Drummond AJ, Xie D, Baele G, Suchard MA.** Posterior summarization in Bayesian phylogenetics using Tracer 1.7. Syst Biol. 2018; 67(5):901–04. https://doi.org/10.1093/sysbio/syy032
- **Ramírez A, Pinilla G.** Hábitos alimentarios, morfometría y estados gonadales de cinco especies de peces en diferentes períodos climáticos en el río Sogamoso (Santander, Colombia). Acta Biolo Colomb. 2012; 17(2):241–58. Available from: http://www.scielo.org.co/scielo.php?script=sci_arttext&pid=S0120-548X2012000200002
- **Reimchen TE, Temple NF.** Hydrodynamic and phylogenetic aspects of the adipose fin in fishes. Can J Zool. 2004; 82(6):910–16. https://doi.org/10.1139/Z04-069
- **Restrepo-Escobar N, Hurtado-Alarcón JC, Mancera-Rodríguez NJ, Márquez EJ.** Variations of body geometry in *Brycon henni* (Teleostei: Characiformes, Bryconidae) in different rivers and streams. J Fish Biol. 2016a; 89(1):522–28. https://doi.org/10.1111/jfb.12971
- **Restrepo-Escobar N, Rangel-Medrano JD, Mancera-Rodríguez NJ, Márquez EJ.** Molecular and morphometric characterization of two dental morphs of *Saccodon dariensis* (Parodontidae). J Fish Biol. 2016b; 89(1):529–36. https://doi.org/10.1111/jfb.12961
- **Restrepo-Escobar N, Yepes-Acevedo AJ, Márquez EJ.** Population genetics of three threatened catfish species in heterogeneous environments of the Cauca River, Colombia. Neotrop Ichthyol. 2021; 19(1):e200040. https://doi.org/10.1590/1982-0224-2020-0040
- **Restrepo-Gómez AM, Rangel-Medrano JD, Márquez EJ, Ortega-Lara A.** Two new species of *Pseudopimelodus* Bleeker, 1858 (Siluriformes: Pseudopimelodidae) from the Magdalena Basin, Colombia. PeerJ. 2020; 8:e9723. https://doi.org/10.7717/peerj.9723
- **Rodgers GM, Kelley JL, Morrell LJ.** Colour change and assortment in the western rainbowfish. Anim Behav. 2010; 79(5):1025–30. https://doi.org/10.1016/j.anbehav.2010.01.017
- **Rohlf FJ, Marcus LF.** A revolution in morphometrics. Trends Ecol Evol. 1993; 8(4):129–32. https://doi.org/10.1016/0169-5347(93)90024-J
- **Ross RM.** Catheterization: a non-harmful method of sex identification for sexually monomorphic fishes. Prog fish cult. 1984; 42 (2):151–52. https://doi.org/10.1577/1548-8640(1984)46<151:C>2.0.CO;2
- **Rosso JJ, Mabragaña E, González Castro M, Díaz de Astarloa JM.** DNA barcoding Neotropical fishes: Recent advances from the Pampa Plain, Argentina. Mol Ecol Resour. 2012; 12(6):999–1011. https://doi.org/10.1111/1755-0998.12010
- **Rozas J, Ferrer-Mata A, Sanchez-Del Barrio JC, Guirao-Rico S, Librado P, Ramos-Onsins SE *et al*.** DnaSP 6: DNA sequence polymorphism analysis of large data sets. Mol Biol Evol. 2017; 34(12):3299–302. https://doi.org/10.1093/molbev/msx248

- **Rubinoff D, Holland BS.** Between two extremes: mitochondrial DNA is neither the panacea nor the nemesis of phylogenetic and taxonomic inference. Syst Biol. 2005; 54(6):952–61. https://doi.org/10.1080/10635150500234674
- **Sidlauskas BL, Mol JH, Vari RP.** Dealing with allometry in linear and geometric morphometrics: A taxonomic case study in the *Leporinus cylindriformis* group (Characiformes: Anostomidae) with description of a new species from Suriname. Zool J Linn Soc. 2011; 162(1):103–30. https://doi.org/10.1111/j.1096-3642.2010.00677.x
- **Scott GR, Johnston IA.** Temperature during embryonic development has persistent effects on thermal acclimation capacity in zebrafish. Proc Natl Acad Sci USA. 2012; 109(35):14247–52. https://doi.org/10.1073/pnas.1205012109
- **Syaifudin M, Bekaert M, Taggart JB, Bartie KL, Wehner S, Palaiokostas C *et al*.** Species-specific marker discovery in tilapia. Sci Rep. 2019; 9(13001). https://doi.org/10.1038/s41598-019-48339-2
- **Scarabotti P, Govezensky T, Bolcatto P, Barrio RA.** Universal model for the skin colouration patterns of neotropical catfishes of the genus *Pseudoplatystoma*. Sci Rep. 2020; 10(12445). https://doi.org/10.1038/s41598-020-68700-0
- **Sugimoto M.** Morphological color changes in fish: Regulation of pigment cell density and morphology. Microsc Res Techniq. 2002; 58(6):496–503. https://doi.org/10.1002/jemt.10168
- **Tamura K, Stecher G, Kumar S.** MEGA11: Molecular evolutionary genetics analysis version 11. Mol Biol Evol. 2021; 38(7):3022–27. https://doi.org/10.1093/molbev/msab120
- **Tipsmark CK, Luckenbach JA, Madsen SS, Kiilerich P, Borski RJ.** Osmoregulation and expression of ion transport proteins and putative claudins in the gill of southern flounder (*Paralichthys lethostigma*). Comp Biochem Phys A. 2008; 150(3):265–73. https://doi.org/10.1016/j.cbpa.2008.03.006
- **Temple NF, Reimchen TE.** Adipose fin condition and flow regime in catfish. Can J Zool. 2008; 86(9):1079–82. https://doi.org/10.1139/Z08-086
- **Untergasser A, Cutcutache I, Koressaar T, Ye J, Faircloth BC, Remm M *et al*.** Primer3-new capabilities and interfaces. Nucleic Acids Res. 2012; 40(15):e115. https://doi.org/10.1093/nar/gks596
- **Valdez-Moreno M, Ivanova NV, Elías-Gutiérrez M, Contreras-Balderas S, Hebert PDN.** Probing diversity in freshwater fishes from Mexico and Guatemala with DNA barcodes. J Fish Biol. 2009; 74(2):377–402. https://doi.org/10.1111/j.1095-8649.2008.02077.x
- **Valbuena-Villarreal RD, Zapata-Berruecos BE, Cruz-Casallas PE.** Reproducción inducida de capaz (*Pimelodus grosskopfii*) con extracto de hipófisis de carpa: reporte preliminar. Orinoquia. 2010; 14(2):133–39. Available from: http://www.scielo.org.co/scielo.php?script=sci_arttext&pid=S0121-37092010000200003
- **Van Der Salm AL, Martínez M, Flik G, Wendelaar Bonga SE.** Effects of husbandry conditions on the skin colour and stress response of red porgy, *Pagrus pagrus*. Aquaculture. 2004; 241(1–4):371–86. https://doi.org/10.1016/j.aquaculture.2004.08.038
- **Vanegas-Ríos JA, Azpelicueta MM, Ortega H.** *Chrysobrycon eliasi*, a new species of stevardiine fish (Characiformes: Characidae) from the río Madre de Dios and upper río Manuripe basins, Peru. Neotrop Ichthyol. 2011; 9(4):731–40. https://doi.org/10.1590/S1679-62252011000400004
- **Vazzoler AEAM.** Biologia da reprodução de peixes teleósteos: teoria e prática. Maringá: Editora da Universidade Estadual de Maringá; 1996.
- **Villa-Navarro FA, Acero A, Cala P.** Taxonomic review of Trans-Andean species of *Pimelodus* (Siluriformes: Pimelodidae), with the descriptions of two new species. Zootaxa. 2017; 4299(3):337–60. https://doi.org/10.11646/zootaxa.4299.3.2
- **Villa-Navarro FA, Usma S, Mesa-Salazar L, Sanchez-Duarte P.** *Pimelodus grosskopfii*, Barbudo. The IUCN Red List of Threatened Species; 2016. https://doi.org/10.2305/IUCN.UK.2016-1.RLTS.T49829828A61473588.en
- **Ward RD, Hanner R, Hebert PDN.** The campaign to DNA barcode all fishes, FISH-BOL. J Fish Biol. 2009; 74(2):329–56. https://doi.org/10.1111/j.1095-8649.2008.02080.x
- **Ward RD, Zemlak TS, Innes BH, Last PR, Hebert PDN.** DNA barcoding Australia's fish species. Philos T R Soc B. 2005; 360(1462):1847–57. https://doi.org/10.1098/rstb.2005.1716

- **Warheit KI, Rohlf FJ, Bookstein FL.** Proceedings of the Michigan Morphometrics Workshop. Syst Biol. 1992; 41(3):392–95. https://doi.org/10.2307/2992576
- **Ye J, Coulouris G, Zaretskaya I, Cutcutache I, Rozen S, Madden TL.** Primer-BLAST: A tool to design target-specific primers for polymerase chain reaction. BMC Bioinformatics. 2012; 13:1–11. https://doi.org/10.1186/1471-2105-13-134
- **Zapata LA, Usma JS.** Guía de las especies migratorias de la biodiversidad en Colombia. Peces. Vol. 2. Bogotá, D. C: Ministerio de Ambiente y Desarrollo Sostenible/WWF-Colombia; 2013.

AUTHORS' CONTRIBUTION

Cristhian Danilo Joya: Conceptualization, Data curation, Formal analysis, Methodology, Software, Validation, Visualization, Writing-original draft, Writing-review and editing.

Ana María Ochoa-Aristizábal: Conceptualization, Data curation, Formal analysis, Software, Validation, Visualization, Writing-original draft, Writing-review and editing.

José Gregorio Martínez: Conceptualization, Data curation, Formal analysis, Methodology, Software, Validation, Visualization, Writing-original draft, Writing-review and editing.

Edna Judith Márquez: Conceptualization, Data curation, Formal analysis, Funding acquisition, Investigation, Methodology, Project administration, Resources, Software, Supervision, Validation, Visualization, Writing-original draft, Writing-review and editing.

ETHICAL STATEMENT

Wild populations were sampled from 2011 to 2014 by Integral S.A. and Universidad de Antioquia, while captive specimens from Piedras (Tarazá, Antioquia Department) and Santa Cruz (Caucasia, Antioquia Department) fish farms were collected by Universidad Nacional de Colombia from 2019 to 2020 under environmental licence # 0155 from the Ministerio de Ambiente, Vivienda y Desarrollo Territorial de Colombia, issued on January 30, 2009.

COMPETING INTERESTS

The author declares no competing interests.

HOW TO CITE THIS ARTICLE

- **Joya CD, Ochoa-Aristizábal AM, Martínez JG, Márquez EJ.** Morphometric and molecular differentiation of *Pimelodus grosskopfii* and *Pimelodus yuma* (Siluriformes: Pimelodidae). Neotrop Ichthyol. 2023; 21(2):e220072. https://doi.org/10.1590/1982-0224-2022-0072

Neotropical Ichthyology

OPEN ACCESS

Official Journal of the
Sociedade Brasileira de Ictiologia
SBI